AMSE JOURNALS –2015-Series: Advances B; Vol. 58; N° 1; pp 67-83
Submitted Dec. 2014; Revised May 31, 2015; Accepted June 20, 2015

2D Gabor Filter for Surface Defect Detection Using GA and PSO Optimization Techniques

* Khwaja Muinuddin Chisti Mohammed, ** Srinivas Kumar S., *** Prasad Gandikota

*Department of ECE, JNTUK University,
Kakinada, A.P., India -533003, (chisti09@gmail.com)
**Department of ECE, JNTUK University,
Kakinada, A.P., India -533003, (samay_ssk2@yahoo.com)
***Department of ECE, SR International Institute of Tech., RR District,
Hyderabad, India, (pgandikota@yahoo.com)

Abstract

Defect detection is one of the main problem domains in automation of industries such as leather, bottle, fruits, textiles etc. The surface defects identification through imaging techniques is becoming extensively used nowadays. One such technique is used is through energy response of Gabor filter convolution of images is used for defects identification. In this method, Gabor parameters are tuned to get minimum energy response of the convolved image using exhaustive search method. However this method is computationally not efficient. To overcome this issue, this paper focuses on using Genetic Algorithms (GA) and Particle Swarm Optimization (PSO) optimization methods to tune Gabor parameters to minimum energy response to increase computation efficiency has been used. The results are reported in the paper. Results obtained from leather images show PSO out performing GA in computational and also results addressed in terms of defect localization.

Key words

Gabor Filter, Genetic Algorithm (GA), Particle Swarm Optimization (PSO), Automation, Defect Detection.

1. Introduction

A defect is considered as area of pixels or pixels that exist other than the original image pixels. Earlier defect detection carried out manually, this method requires experienced worker for the identifications, which is cost effective. Automation using digital image processing has advantages in both accuracy and robustness. The later one is important because manual inspection worker get drowsy, lazy, etc., in continuous inspection while the automatic system gives result at same accuracy as that of first image to the last image. The accuracy of defect identification depends on the type of the algorithm used. There are number of algorithms developed for the texture defect detection and classification. Texture analysis mainly classified into two categories, namely statistical and structural.

Most of the automatic defect detection methods are focused on the surfaces like steel bridge coating rust [16], wood inspection [18], patterned textures [13], leather surface [8] [25], skin lesions [4], granite tiles [1], ceramic tiles [3], cylindrical pipe [21], bones [11], etc. In all these works texture defects generally have different features than the homogeneous background and are implemented in both spatial and frequency domains. The spatial domain methods such as histogram based [6] [14] [15], gray level co-occurrence matrix GLCM and Harlick features [17], similarity measures, etc., are sensitive to the noise & the GLCM need more computation, on the other hand frequency domain methods are less sensitive to noise and the features can be extracted from Fourier Transform, Gabor Transform [2] [7] [26], Wavelet Transform [10], etc. A hybrid method that combine both statistical and structural features for texture representation is presented by et.al Ganesan [5]. A good review papers in this area are surface defect detection using texture analysis techniques [24], monitoring and grading of tea by computer vision [19], Automated fabric defect detection [12].

The basic work of et.al Tsai [22], defect detection in colored texture surface using Gabor filter, where the defect detection carried using the energy response of Gabor filter convolution with the image. In this work the Gabor parameters are tuned to get minimum energy response of the convolved image using exhaustive search method which is computationally inefficient. This can be improved drastically using GA and later work of this paper shows PSO outperform the GA optimization in terms of minimum energy response and computational efficiency.

The mathematical representation of 2D Gabor filter, filtering of gray/color image using the 2D Gabor filter and the computation of energy are discussed in section 2. In the section 3, defect detection mechanism used in this work is show cased. In the section 4, Optimization of the energy using three different methods presented and the PSO proposed in this work outperforms over traditional exhaustive search and the GA. Section 5, simulation results obtained on a PC installed with MATLAB are discussed.

2. Gabor Filter

In 1946, Dennis Gabor proposed Gabor expansion which is a type of Short Time Fourier Transform. Using an overlapped or non-overlapped sliding window, Gabor Transform mask the local input signal and transforms it into frequency domain.

2.1 Mathematical representation of 2D Gabor Filter

A 2D Gabor filter obeys separable property. This indicates that a 2D Gabor filter can be obtained by multiplying two 1D signals of x and y directions respectively. Thus the obtained Gabor filter is multiplied with the signal of a symmetric sliding window, and then transforms it to the frequency domain to obtain the transformed image. A 1D Gabor transform is obtained by multiplying Gaussian function with sinusoidal signal. The equations (1) and (2) represents the 1D Gabor transform.

$$G_x = g_x * \exp(j\omega_x * x) \tag{1}$$

$$G_y = g_y * \exp(j\omega_y * y) \tag{2}$$

where G_x and G_y are the 1D Gabor transforms with g_x and g_y as Gaussian functions in x and y directions given in equation (3) and (4) respectively.

$$g_x = \frac{1}{\sqrt{2\Pi}\sigma_x} \exp\left(\frac{-x^2}{2\sigma_x^2}\right) \tag{3}$$

$$g_y = \frac{1}{\sqrt{2\Pi}\sigma_y} \exp\left(\frac{-y^2}{2\sigma_y^2}\right) \tag{4}$$

where σ_x and σ_y are scale parameters of a Gaussian function. The frequency components ω_x and ω_y in equation (1) and (2) are obtained using equation (5) and (6) respectively.

$$\omega_x = \omega_0 * \cos(\alpha * f) \tag{5}$$

$$\omega_y = \omega_0 * \sin(\alpha * f) \tag{6}$$

where f is frequency of the signal and α is orientation of the signal with $\omega_0 = 0.1 * (\Pi/2)$. Now using separable property, a 2D Gabor Transform is obtained by using the equation (7).

$$G_{\sigma,\mathrm{f},\alpha}(x,y) = G_x * G_y \tag{7}$$

where $G_{\sigma,f,\alpha}(x,y)$ is a 2D complex quantity with x, y varying through the filter dimensions with the parameters σ_x, σ_y, f, and α.

Gray image Gabor filter output is the convolution of Gabor filter and input image. The gray image energy response is the squared modulus of filter output, which is computed by using the equation (8), as described by et.al Tsai [22].

$$E_{gray(\sigma,f,\alpha)}(x,y) = G^2_{R(\sigma,f,\alpha)}(x,y) + G^2_{I(\sigma,f,\alpha)}(x,y) \tag{8}$$

where G_R and G_I are real and imaginary parts of filter output. Fig. 1 shows the variant of Gabor filter with respective to parameter selection.

In the gray image, gray level information is directly used where as in color image, two chromatic features (h_{ab} and C^*_{ab}) are used to represent the image $I=h_{ab}+jc^*_{ab}$ for applying Gabor

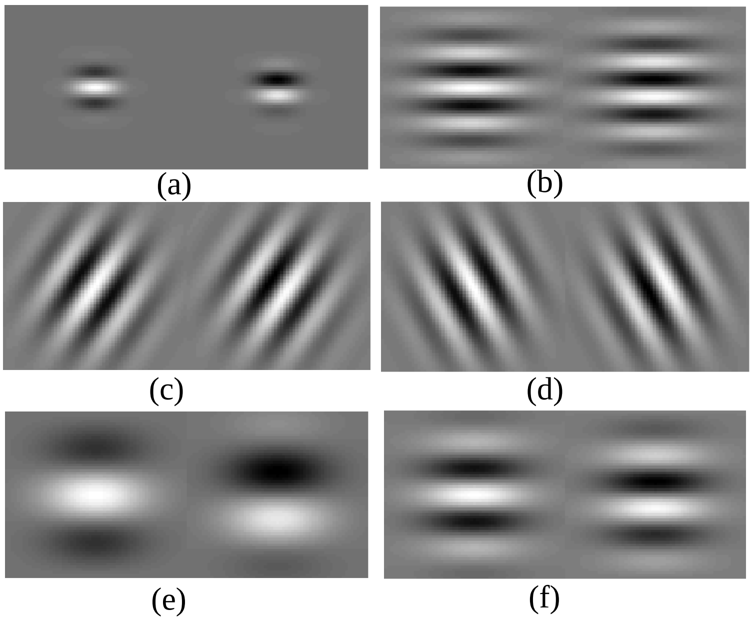

filter. The features are extracted using CIE-L*a*b* color space [22].

Fig. 1. Gabor filter variants with (a) σx=5; σy=5; θ=0o; f=; (b) σx=15; σy=12; θ=0o; f=3; (c) σx=15; σy=12; θ=45o; f=3; (d) σx=15; σy=12; θ=90o; f=3; (e) σx=15; σy=12; θ=0o; f=1; (f) σx=15; σy=12; θ=0o; f=2;

Color Gabor filter output is the convolution of Gabor filter with the complex number $h_{ab}+jc^*_{ab}$, which also has varying parameters σ_x, σ_y, f and α same as gray image. The color image energy response is the squared modulus of filter output. , which is computed by using the equation (9).

$$E_{color(\sigma,f,\alpha)}(x,y) = C^2_{R(\sigma,f,\alpha)}(x,y) + C^2_{I(\sigma,f,\alpha)}(x,y) \quad (9)$$

3. Proposed Defect Detection Mechanism

A defect in an image is defined as the unknown characteristic that appears in the image other than the original image. A defect free image is an image which is similar to the original image. The defect detection is carried out in two stages namely training stage and testing stage.

In the training stage, the Gabor filter parameters are chosen such that the energy response of the color or gray image samples (E_{color} or E_{gray}) when convolved with Gabor filter is near to zero (minimum) for a defect free sample of the input image. In this work, the energy response is minimized using optimization techniques with respective homogenous texture surface, plain textures and periodic patterns.

In testing stage, an unknown image is marked as defective or defect free depending up on the energy response at each and every sample of the unknown image. Samples can be taken as overlapped or non-overlapped windowing. In this paper, results are obtained by considering overlapped windowing since the overlapped windowing gives good localization of the defect but at a cost of computation. If the energy response of the image sample is near to training sample energy response then the sample is marked as defect free otherwise it is marked as defective sample which yields a varyingly higher energy responses.

As a result, the complex defect detection problem of the colored image is simplified and the results obtained in the form of black and white image shows the successes of the detection mechanism where a black is marked as non-defective pixel and white is marked as defective pixel. The entire process of filtering is summarized using the flow chart as shown in the Fig. 2.

4. Optimization of Energy Response

Acquiring the minimum energy response requires four filter parameters σ_x, σ_y, f and α properly tuned and it can be done using exhaustive searching method that results in computationally inefficient. Optimization techniques are used to minimize or maximize the fitness function by selecting suitable parameters. A good review paper outlines set of optimization techniques et.al Worden [23]. These techniques are used to get optimum solution iteratively with less computation complexity. As described above the fitness function here is the energy function E_{gray} or E_{color} for gray/color images. The optimum condition here is to minimize energy function and the problem is stated as minimization. The parameters are varied such that the energy gets minimized. The parameters in this problem are varied as $\sigma_{min} \leq \sigma x, \sigma y \leq \sigma_{max}$, $f_{min} \leq f \leq f_{max}$, and $0^o \leq \alpha \leq 180^o$.

A typical values for the selected textures after many experiments on different samples varies as $f_{min} = 1$, $f_{max} = R$ (width window), $21^o \leq \alpha \leq 30^o$, $1 \leq \sigma x, \sigma y \leq 20$ with fitness function as E_{gray} or E_{color}. This problem domain is known to be multi variables unconstraint optimization problem.

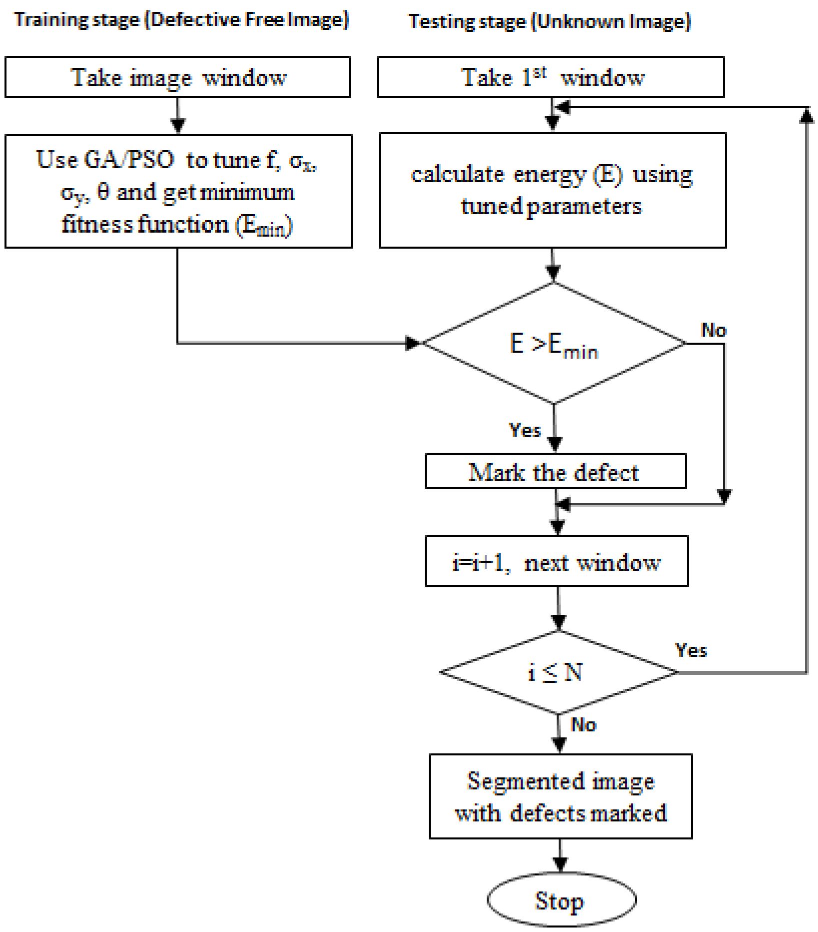

Fig. 2. Flow chart for training and testing stage of defect detection mechanism (N=total number of windows)

4.1 Optimization using Genetic Algorithm

Genetic algorithm is an evolutionary technique that optimally solves the problem automatically. In recent, a large part of automatic machine learning algorithms involve the use of genetic algorithm. It uses the biological evolution to solve many complex problems with relatively less computational affects [9]. This work is basically a multi variable unconstraint optimization problem where the algorithm search for the optimal solution by simultaneously varying all the four parameters and maintaining the solution with in a feasible search area. The genetic algorithm is summarized using the flow chart as shown in the Fig. 3. The initial population is iteratively processed using the three operators until the termination condition is met. One iteration of these three operators is known as a generation.

In this application, maximum population size of 20, and a four variables are randomly coded in binary strings in their respective intervals and the continuous values obtained using $var = var^{lowlt} + (var^{highlt} - var^{lowlt}) * dec(binary\ var)/(2^b - 1)$. Where b represents number of bits to variable (6bits), var^{lowlt}, var^{highlt} represents lower and higher limits of the variable and dec(bin)= decimal equivalent of binary value of the variable. These continuous values used to obtain the fitness function (Emin) values for initial population as in the Table 1. The four variables each of 6bits form a bit string of 24bits. In the initialization of GA set gen=0; max. gen. =200, max. population size=20, selection probability=0.5, mutation probability Pm=0.15.

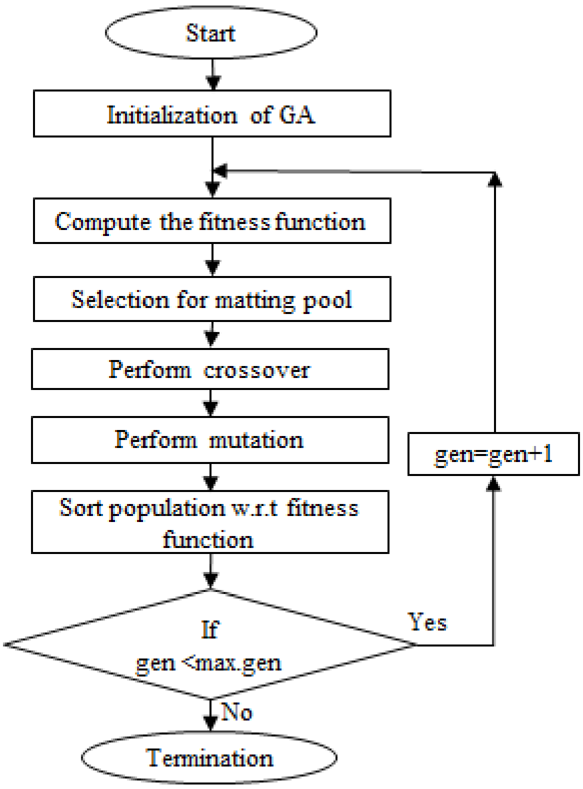

Fig. 3. Optimization using Genetic Algorithm

Selection operator: Selects good strings from current population and are assigned large number of copies to form mating pool in a probabilistic way. Selection probability 0.5 is used in the program. This means 10 out of 20 population are preserved and 10 participate in mating. Total No. of Mating's= (20-10)/2=5. The population numbers that are selected for matting and the mating1 and mating2 chromosomes used for crossover at bit position are also shown in last two columns in the Table 2.

Table 1: Initial parameters and its fitness values for gray image

Pop. No.	σ_x	σ_y	α	f	Fitness E_{min}	Initial Population Sorted w.r.t fitness	
						σ_x σ_y α f	Fitness E_{min}
1	100000	101011	111011	011000	1.050e-009	011110 001101 101110	2.122e-021
2	011110	001101	101110	100010	2.122e-021	100010	3.216e-016
3	101100	100000	001000	101001	2.804e-007	010000 100110 100110	3.441e-012
4	111010	010010	101010	111100	5.661	010001	5.104e-012
5	000100	010011	010000	011011	1.974e-008	010101 101100 000000	1.119e-011
6	101000	010101	111010	111110	518.26	000011	1.765e-011
7	101000	011000	011011	010110	1.154e-010	010100 110111 101010	1.154e-010
8	010000	100110	100110	010001	3.216e-016	010000	1.050e-009
9	010101	101100	000000	000011	3.441e-012	010101 101010 001101	1.974e-008
10	010100	000000	110000	010011	7.536e-008	110000	7.536e-008
11	101100	000000	101101	101001	0.005066	001100 011000 111010	2.498e-007
12	011001	101010	011100	101111	8.733e-007	101100	2.804e-007
13	010101	101010	001101	110000	1.119e-011	101000 011000 011011	8.733e-007
14	010100	110111	101010	010000	5.104e-012	010110	8.801e-007
15	110110	111011	000110	001101	3.025e-005	100000 101011 111011	9.780e-007
16	001100	011000	111010	101100	1.765e-011	011000	3.025e-005
17	000011	001100	000001	110001	0.0003771	000100 010011 010000	0.0003771
18	110101	011011	001110	110010	2.498e-007	011011	0.005066
19	101111	110100	010000	000011	8.801e-007	010100 000000 110000	5.661
20	010101	101000	110011	010010	9.780e-007	010011	518.26
						110101 011011 001110	
						110010	
						101100 100000 001000	
						101001	
						011001 101010 011100	
						101111	
						101111 110100 010000	
						000011	

						010101 101000 110011 010010	
						110110 111011 000110 001101	
						000011 001100 000001 110001	
						101100 000000 101101 101001	
						111010 010010 101010 111100	
						101000 010101 111010 111110	
Minimum cost= 2.122e-021 , With pop No.=2, Average cost=26.196,							

Table 2: Selection for making mating pool

S.No	Chro mo. No.	Probabilities	Cumulative Interval	Rand1 seq. five	Mating1 Chromos ome	Rand2 seq. five	Mating2 Chromos ome	Random No. between 1 to 24 for cross over bit pos.
1	10	0.18182(10/55)	0-0.18182	0.1109	**1**	0.87988	**7**	10
2	9	0.16364 (9/55)	0.18182-0.34545	0.41878	**3**	0.33109	**2**	17
3	8	0.14545 (8/55)	0.34545-0.49091	0.62391	**5**	0.07698	**1**	12
4	7	0.12727 (7/55)	0.49091-0.61818	0.17774	**1**	0.49662	**4**	21
5	6	0.10909 (6/55)	0.61818-0.72727	0.8395	**7**	0.38005	**3**	4
6	5	0.090909(5/55)	0.72727-0.81818					
7	4	0.072727(4/55)	0.81818-0.89091					
8	3	0.054545(3/55)	0.89091-0.94545					
9	2	0.036364(2/55)	0.94545-0.98182					
10	1	0.018182(1/55)	0.98182-1					
	∑=55							

Crossover: New child string is formed by selecting two parent strings from the mating pool and exchanging some portion of the bits between them, excepting that the formed child string is a good string. This is known as single point crossover operator which is used in this application. If the formed child is a bad string it gets eliminated in successive iterations. Crossover applied at the bit position as in last column of Table 2 between mating chromosomes as in Table 3. This shows chromosome strings 1 and 7 crossover at bit position 10 to generate new child strings 11 and 12. Similarly other populations are generated.

Table 3. Crossover between chromosomes 1 and 7 to generate new chromosomes 11 and 12

Pop No.	σ_x σ_y α f	New Pop No.	After crossover
1 7	011110 0011 01 101110 100010 101000 0110 00 011011 010110	11 12	011110 0011 00 011011 010110 101000 0110 01 101110 100010

Mutation: It is used to perform local search of solution around the selected string. A bit of the string is complemented based on the mutation probability (Pm). In this paper Pm selected to be 0.15. A population number is selected in between (1 to 20) randomly and a random number is generated in between (1 to 24) indicating bit positions. This bit position of the selected population is complemented to get muted population. Table 4 shows bit string before and after mutation at the bit position 3 in the 3rd population. Total mutation considered as (max. pop-1) x 24xPm =69.

Table 4. Chromosomes before and after mutation.

Pop No.	Before mutation	After mutation
3	01**0**101 101100 000000 000011	01**1**101 101100 001100 000011

Termination: GA is terminated if the maximum number of generations or iterations are completed or maximum number of strings in the population are same. Here in this work maximum generations chosen to be 200. Executing three operators for one time is considered to be one generation.

The Table 5 shows the parameters after selection and mutation at the end of first generation with sorted population w.r.t fitness. These parameters are initial input population to next generation. The Fig. 4 shows the convergence curve of binary GA for energy minimization by tuning four parameters of gray image.

4.2 Optimization using Particle Swarm Optimization (PSO)

A computational method to optimize the fitness function iteratively to improve the required solution with respective to the given parameters. In this the particles are moved around the search space using a mathematical formula around the particle's position and velocity [27]. In this work, PSO is simulated using parameter max iteration = 150, r1, r2 random numbers in between (0 to 1), C=1, social and cognitive parameters as c1=1.5, c2=1.5 and constriction factor C=1.

Table 5. Sorted parameters w.r.t fitness after one generation

Pop No.	σ_x σ_y α f	Fitness Emin
1	001110 001000 110000 010011	4.975e-023
2	011110 001101 101110 100010	2.122e-021
3	011110 001111 101010 010000	7.926e-018
4	010000 100110 101110 010001	5.455e-016
5	001001 011000 111011 010111	3.334e-015
6	111100 001100 011011 000110	1.008e-014
7	010100 101100 000000 001011	9.120e-012
8	010100 110111 111000 110100	1.52e-011
9	000100 010000 111010 101100	2.940e-011
10	010111 101000 011111 010111	9.879e-011
11	101001 011000 000000 100011	1.809e-010
12	011101 101100 001100 000011	1.834e-009
13	010101 101000 111010 110010	2.291e-009
14	010111 011110 001001 110100	4.192e-009
15	111010 011101 101110 100010	1.562e-008
16	000100 010011 010000 011011	1.974e-008
17	100000 101011 111001 000011	4.775e-008
18	110101 101010 001101 101001	2.014e-006
19	010001 101100 100111 101001	0.0070851
20	000100 110101 111110 100111	0.021583

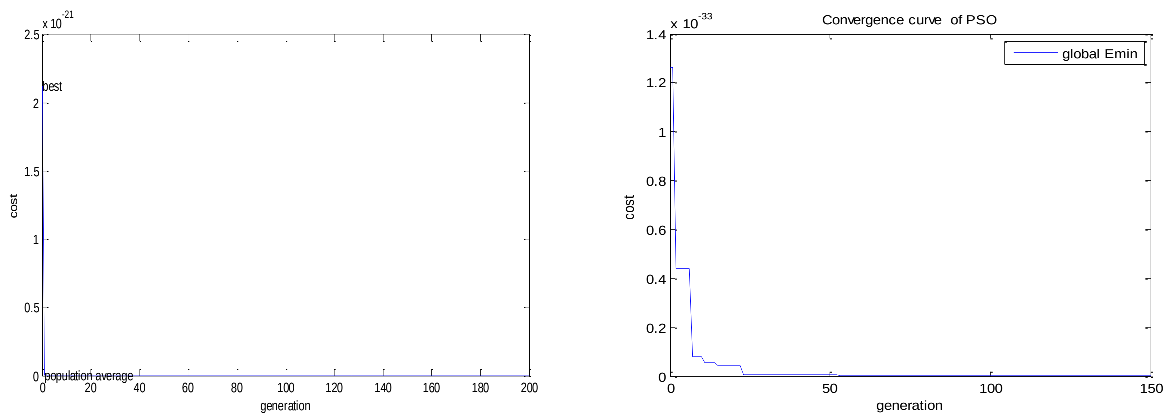

(a) (b)

Fig. 4. Convergence curve of (a) GA (b) PSO

Iterative steps of PSO as follows:

Step1: Population size=50, randomly initialize four parameters f, σ_x, σ_y ,θ (i=1,2,3,4) with same variables interval for higher and lower limits ($Var^{lowlt}(i)$, $Var^{highlt}(i)$) using $Var(i)=Var(i)*(Var^{highlt}(i)- Var^{lowlt}(i))+ Var^{lowlt}(i)$.
Step2: Calculate Initial Velocities for each variables: $vel^{lowlt}(i) = -1*(Var^{highlt}(i)- Var^{lowlt}(i))$ and $vel^{highlt} = (Var^{highlt}- Var^{lowlt})$, $velInt(i)=vel(i)*(vel^{highlt}(i)- vel^{lowlt}(i))+ vel^{lowlt}(i)$, for each variable.
Step3: Calculate Fitness function for each population (E_{gray} or E_{color}), consider them as localvar minima's for each variable and find minimum Fitness, mark it as initial gobalvar minima and mark it as best population in the initial population.
Step4: Iterations

Inertia weight w = (max Iteration – current Iteration)/ max Iteration;
Update velocity vel (i) = C*(w*vel(i)+c1*r1*(localvar(i)-var(i)) + c2*r2*(globalvar-var(i)));
Update position var (i) = var(i) + vel(i);
Calculate fitness function for updated position
Update best local positions (localvar(i)) as local position if fitness < previous fitness
Update globalvar(i) as variable values of minimum fitness function.

Repeat Step 4 until max iteration reached.

The same image and the same parameters are optimized using PSO. The work is simulated for 150 to 200 iterations several times and it is observed that PSO gives the minimum energy than the GA with the same conditions on parameters at less computational time. Fig. 4 shows the convergence curve of PSO.

The Table 6 shows the three different methods used to optimize the energy with respective to the same parameter boundaries. From the table it is seen that the PSO is having minimum fitness.

Table 6. Comparison of optimal solution using three methods

Optimization	Remark	Values of Optimal Parameters				Fitness Emin gray
		σ_x	σ_y	A	*F*	
Exhaustive searching	One unit interval	4	4	23	29	3.746e-36
GA	200 gen.	4.016	3.111	24.429	25.397	1.142e-37
PSO	150 Iterations	3.103	18.406	22.673	23.153	7.618e-39

5. Experimental Results

The Images in this work are 360x360 pixels. The three sizes of the windows are used for the experimental work are 6x6, 15x15, 60x60 pixels. The defect can be detected easily using all the three windows but the exact defect localization is obtained with small size window and a larger window size will result in poor resolution and a smaller window would leads to higher computation.

The selection of window size is important in localizing the defect, this was addressed by Tolba[20] adaptive sizing of the sliding window is proposed. The Fig. 5 shows the filtering color image and Fig. 6 shows filtering of gray image using 2D Gabor filter with varying window size for the same image. It is clearly seen from the results the proper window size helps in achieving good localizing the defect.

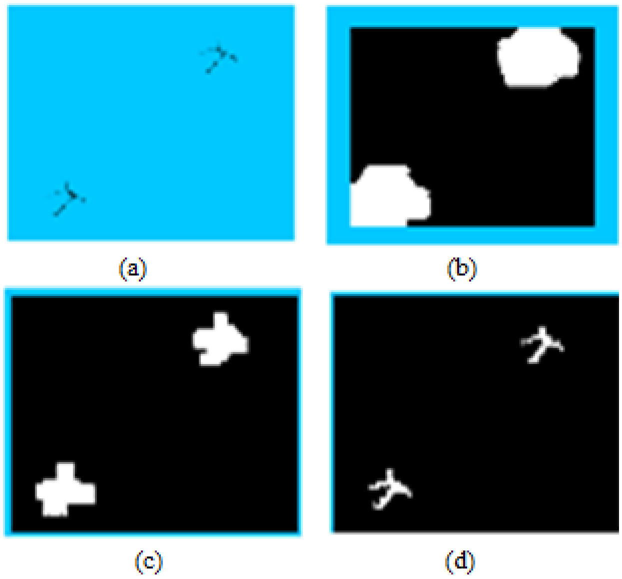

Fig. 5. Color Gabor filter results (a) Defected input color image with two cracks (b) Output image for window size 60X60 (c) Output image for window size 15X15 (d) Output image for window size 5X5

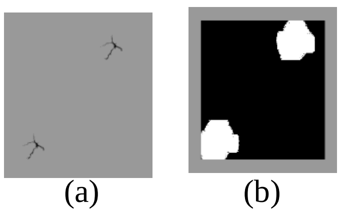

Fig. 6. Gray Gabor filter results (a) Defected input gray image with two cracks (b) Output image for window size 60X60

The choice of a proper window size is most important for periodic patterns of homogeneous texture. In Fig. 7 a periodic pattern is filtered using a non-overlapping window of size propositional to the periodicity of the pattern is used.

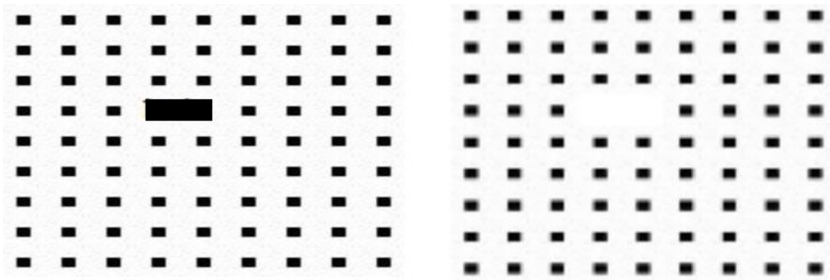

(a) (b)

Fig. 7. (a) Defected pattern of periodic image and (b) Output image after defect detection

Table 6 clearly shows the optimization methods, PSO optimization gives the minimum energy response of 7.618e-39 for the image considered in comparison with the GA optimization. This energy is used as the threshold for classifying the defective image. In this way the Gabor tuned filter for non-defective homogeneous Color or Gray images is used to convolve with the unknown image. The unknown image can be stated as defective if the tuned Gabor filter response exceed the threshold level else considered as non-defective image.

Conclusion

The defect detection and the localization of the defect is addressed with respective the homogeneous textures, periodic textures for gray and color images. In training phase, 2D Gabor filter convolved with defect free image window by tuning the four parameters of the filter using three different methods with in the same parameter limits to obtain minimum energy response is presented in this work. In this way a tuned Gabor filter is obtained and its energy is used as threshold for detecting the defects. In testing phase, when an unknown image window is convolved with tuned Gabor filter of the training stage, if energy responses is greater than the threshold it is marked as defect else non-defective. From the results it shows that the minimum energy response of 7.618e-39 is obtained with PSO compared to the 1.142e-37 energy response of GA. Experiments carried out on different homogeneous leather surfaces and pattern images, the result of energy response of the PSO is minimum than GA and PSO tuned Gabor filter results shown in this work localize the defect to the industry requirements depending on the window size and type of the window chosen. In this work an overlapping window is chosen for better localization of defect in homogeneous color and gray images with different window sizes and a non-overlapping window of size equal to the periodicity of the periodic patterned image is chosen to detect defects. It is shown that the result obtained with these considerations not only detect the defect but also localize defect. The fixing of the window size is the main consideration in localizing the defect is addressed and work can be extended for sizing the window adaptively. Automatic selection of window can be implemented to improve the performance.

Acknowledgment

The authors wishes to acknowledge Dr. Chellapa Muralidharan, Scientist F, Central Leather Research Institute (CLRI), Adyar, Chennai, India for providing the leather images and necessary support.

References

[1] Bianconi F., Gonzalez E., Fernandez A., and Saetta S.A., "Automatic classification of granite tiles through colour and texture features," Expert Systems with Applications, Vol. 39, pp. 11212–11218, 2012.

[2] Bissi L., Baruffa G., Placidi P., Ricci E., Scorzoni A., and Valigi P. "Automated Defect Detection in Uniform and Structured Fabrics using Gabor Filters and PCA,"J. Vis. Commun. Image R, Vol. 24, pp. 838–845, 2013.

[3] Boukouvalas C., Kittler J., Marik R., and Petrou M., "Color Grading of Randomly Textured Ceramic Tiles Using Color Histograms," IEEE Transactions on Industrial Electronics, Vol. 46, No. 1, pp. 219 – 226, 1999.

[4] Cavalcanti P. G., Scharcanski J., and Baranoski G.V.G., "A two-stage approach for discriminating melanocytic skin lesions using standard cameras," Expert Systems with Applications-Elsevier, Vol. 40, pp. 4054–4064, 2013.

[5] Ganesan L., Umarani C., and Radhakrishnan S., "A combined statistical and structural approach for texture representation and its characterization," AMSE Journal, Advances B, Vol. 51, N° 1, pp. 65, 2008.

[6] Iivarinen J., "Surface Defect Detection with Histogram- Based Texture Features," Intelligent Robots and Computer Vision XIX: Algorithms, Techniques, and Active Vision, SPIE, Boston MA, USA, Vol. 419, pp. 140-145, 2000.

[7] Kumar A, and Pang G., "Defect Detection in Textured Materials using Gabor Filters," IEEE Transactions on Industry Applications, Vol. 38, pp. 2, 2002.

[8] Kwak C., Ventura J. A., and Tofang K., "A Neural Network Approach for Defect Identification and Classification on Leather Fabric," Journal of Intelligent Manufacturing Vol. 11, pp. 485-499, 2000.

[9] Kalyanmoy Deb, Otimization for engineering design: Algorithms and examples, Publication PHI Learning Pvt. Ltd, 2004

[10] Li W.C., and Tsai D.M., "Wavelet-based defect detection in solar wafer images with inhomogeneous texture," Pattern Recognition-Elsevier, Vol. 45, pp. 742–756, 2012.

[11] Meziane A., Bachari N. E. I., and Naili Q., "Image processing and detection of cold and hot spots in bone scintigraphy," Journal of AMSE, Lectures on Modeling and Simulation, Vol. 5, Issue 2, pp. 135, 2004.

[12] Ngan H.Y.T., Pang G.K.H, and Yung N.H.C., "Automated Fabric Defect Detection—A review," Image and Vision Computing, Vol. 29, pp. 442–458, 2011.

[13] Ngan H.Y.T. and Pang G.K.H., "Regularity Analysis for Patterned Texture Inspection," IEEE Transactions on Automation Science and Engineering, Vol. 6, No. 1, 2009.

[14] Otsu N., "A Threshold Selection Method from Gray-Level Histograms," IEEE Transactions on Systems, Man, and Cybernetics, Vol. 9, No. 1, 1999.

[15] Sheeba O. and Sukesh Kumar A., "Image enhancement and histogram equalization in the detection of drusen deposit in human retina," AMSE Journal, Modelling C, Chemistry, Geology, Environment and Bioengineering, Vol. 71, Issue 1, pp. 12, 2010.

[16] Shen H.K., Chen P.H., and Chang L.M., "Automated Steel Bridge Coating Rust Defect Recognition Method Based on Color and Texture Feature," Automation in Construction, Vol. 31, pp. 338–356, 2013.

[17] Siéler L., Tanougast C., and Bouridane A., "A Scalable and Embedded FPGA Architecture for Efficient Computation of Grey Level Co-occurrence Matrices and Haralick Textures Features," Microprocessors and Microsystems, Vol. 34, pp. 14–24, 2010.

[18] Silv´en O., Niskanen M., Kauppinen H., "Wood inspection with non-supervised clustering," Machine Vision and Applications, Springer-Verlag, Vol. 13, pp. 275-285, 2003.

[19] Singh G.G., Kumar A., and Agarwal R., "Monitoring and Grading of Tea by Computer Vision -A review," Journal of Food Engineering, Vol. 106,pp. 13–19, 2011.

[20] Tolba A.S., "Fast Defect Detection in Homogeneous Flat Surface Products," Expert Systems with Applications, Vol. 38, pp. 12339–12347, 2011.

[21] Touabti M. C. A. , Guellal M., and Abdesselam H., "Defect detection in a cylindrical pipe. Application to a natural gas pipeline," Journal of AMSE, Lectures on Modeling and Simulation, Serie A, Kuala Lumpur (Malaysia), Vol. 7, Issue1, pp. 100, 2006.

[22] Tsai D. M., Lin C. P., and Huang K.T., "Defect Detection in Colored Texture Surfaces using Gabor Filters," The Imaging Science Journal, Vol. 53, pp. 27-37, 2005.

[23] Worden K., Staszewski W. J., and Hensman J.J., “Natural Computing for Mechanical Systems Research: A tutorial overview,” Mechanical Systems and Signal Processing, Vol. 25, pp. 4–111, 2011.

[24] Xie X, “A Review of Recent Advances in Surface Defect Detection using Texture Analysis Techniques,” Electronic Letters on Computer Vision and Image Analysis, 7(3), pp. 1-22, 2008.

[25] Yeh C. and Perng D.B. “Establishing a Demerit Count Reference Standard for the Classification and Grading of Leather Hides,” Springer-Verlag London Limited, On International Journal of Advanced Manufacturing Technology, Vol. 18, pp. 731–738, 2001.

[26] Zhang Y., Lu Z., and Li J., “Fabric Defect Detection and Classification Using Gabor Filters and Gaussian Mixture Model,” Asian Conf. Computer Vision (ACCV2009), Part II, Lecture Notes in Computer Science Vol. 5995, pp. 635–644, 2010.

[27] Gopi E.S. Algorithm Collections for Digital Signal Processing Applications Using Matlab, Springer, ISBN 978-1-4020-6409-8 (HB), 2007.